

# Experimental investigation of the current distribution in Mohler cell and Rotating Cylinder Hull cell

Manida Teeratananon,<sup>a</sup> Kejvalee Pruksathorn,<sup>a</sup> Somsak Damronglerd,<sup>a\*</sup>  
Franck Dupuy,<sup>b</sup> Hugues Vergnes,<sup>b</sup> Bernard Fenouillet<sup>c</sup> and Patrick Duverneuil<sup>c</sup>

<sup>a</sup> Department of Chemical Technology, Faculty of Science, Chulalongkorn University, Bangkok, Thailand.

<sup>b</sup> Institut National Polytechnique de Toulouse, 6 Allée Emile Monso 31029 Toulouse Cedex 4, France.

<sup>c</sup> Ecole Nationale Supérieure des Ingénieurs en Arts Chimiques et Technologiques, 118, route de Narbonne 31077 Toulouse Cedex 4, France.

\* Corresponding author, E-mail: dsomsak@sc.chula.ac.th

Received 26 Nov 2003

Accepted 31 Aug 2004

**ABSTRACT:** Two electroplating test cells have been proposed and tested to analyze the performance of plating solutions by studying the reaction distribution on the cathode during deposition of copper electrolyte. The first one is a modified Mohler cell composed of a rectangular electrolytic cell with forced electrolyte flow and two flat electrodes (an insulating separator is inserted between the cathode and anode). This screen modifies the electric field distribution, and leads to a non-uniform current distribution or deposit thickness on the cathode panel. The other is a rotating cylinder Hull cell consisting of an inner rotating cylinder electrode coaxial with a stationary outer insulating tube to produce a non-uniform current distribution along the length of a cylinder cathode. These kinds of cells are developed to overcome the absence of a controlled mass transport condition associated with the tradition Hull cell. From the experimental results, it appears that the rotating cylinder Hull cell is a better device to characterize and control electrolytic bath, while the experimental errors of the continuous Mohler cell were accounted for using simulation.

**KEYWORDS:** Mohler cell, Rotating Cylinder Hull cell, electroplating test cell, current distribution

## INTRODUCTION

Electrochemical plating is used to give a particular property to a component. This can be a decorative (e.g. silver, gilding), physical or mechanical property (e.g. hard chromium), or protection against corrosion (e.g. nickel and chromium). It is often purposely carried out under non-uniform current distribution, using electroplating test cells. In a single experiment, electroplaters can be used to study the effect of a wide range of current densities on deposit morphology and composition, saving time and cost in the investigation.

The Hull cell<sup>1</sup> (Fig. 1), developed by Hull in 1939, is a versatile tool to analyze the performances of plating solutions. It is a trapezoidal structure where the cathode is placed at an oblique angle with respect to the anode. The cell allows variable solution resistance between the electrodes such that metals can therefore be deposited over a wide range of current densities. The Hull cell can also provide deposit properties at various current densities on a single test panel, making it a useful tool for quality control in electroplating.

Although it is useful in many applications, the Hull cell plating mass-transport conditions are variable and it is often necessary to stir the electrolyte vigorously to

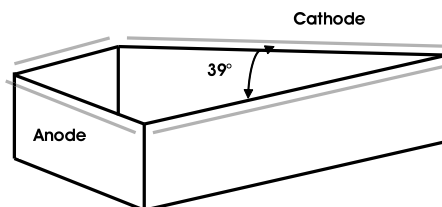


Fig 1. The traditional Hull cell.

improve mass transfer condition at the electrode surface. Usually, a magnetic stirrer or air agitation near the cathode is employed, but neither provides reproducible mass transfer. In order to overcome this, numerous studies have been made to improve mass transfer in the Hull cell or other types of test cells<sup>2-5</sup>. In these studies, a rotating electrode, in the form of a cone or cylinder, was employed to provide well-defined hydrodynamic conditions and increase the magnitude of operating cathodic current densities. Lu<sup>†</sup> proposed several designs using conical and cylindrical electrodes. The described cell configurations, however, were either empirical or of complex geometry and therefore, had limited applicability. In this investigation, a modified

Mohler cell is adopted, consisting of a rectangular cell with forced electrolyte flow, and two electrode plates has been developed to provide well-defined hydrodynamic conditions. The insulating screen placed between the cathode and anode modifies the electric field in such a way to produce a variation of current density across the cathode plate. The continuous flow provides a stable hydrodynamic flow. The aim of this work is to design and to build a modified Mohler cell that is capable to reproduce constant hydrodynamic conditions at the cathode surface by forcing electrolyte flow parallel to the electrode.

## MATERIALS AND METHODS

Regardless of the purpose of the plating operation, the distribution of an electrode deposit on a substrate is determined by the local current density at each point along the cathode surface and by the cathodic current efficiency (at that one applied average current density). The primary current distribution depends only on the geometry of the electrochemical cell. It is independent of the properties of the solution. The distortion of the primary current distribution by polarization at the electrode results in the secondary current distribution<sup>6</sup>.

The uniformity of the secondary current distribution depends on cell geometry and on the value of the Wagner number,  $Wa$ . Wagner number expresses the ratio of the polarization resistance at the electrode surface ( $d\eta/di$ ) and the ohmic resistance ( $\rho \cdot L$ ) of the electrolyte, where  $\eta$  is the overpotential and  $d\eta/di$  is the slope of the potential current curve.

$$Wa = \frac{d\eta/di}{\rho \cdot L} = \frac{\beta_c \cdot k}{i_{avg} \cdot L} \quad (1)$$

Here  $\rho$  is the electrolyte resistance,  $k$  is the electrolyte conductivity ( $k=1/\rho$ ),  $i_{avg}$  is the average current density,  $\beta_c$  is cathodic Tafel constant, and  $L$  is a characteristic length of the system. As  $Wa$  is increased, the current distribution becomes more uniform. The primary current distribution corresponds to  $Wa$  value near zero, and is attained when  $i_{avg}$  are high. In order to study the primary current distribution ( $Wa$  tends towards zero), large cell dimensions and/or high current densities are required<sup>7</sup>. Secondary current distribution is always more uniform than the primary current distribution. Under conditions where the polarization resistance becomes dominating, *i.e.*, when the  $Wa$  tends towards infinity, the current distribution becomes more perfectly uniform, and less dependent of geometry. Finally, in presence of significant mass transports (and its polarization effects), a tertiary current distribution

often prevails. The current distribution in this case depends on both the potential distribution and mass transport.

The local current density depends not only on charge transfer kinetics, but also on mass transport and current distribution. Thus, all three phenomena must be taken into account in modeling metal deposition and in experimental design. The laboratory studies on metal deposition should therefore be carried out under controlled hydrodynamic and current distribution conditions at the cathode.

## Mohler Cell

Mass transfer conditions could have a strong effect on deposit properties. Accordingly, providing reproducible mass transfer conditions, which can result from a well-defined hydrodynamic flow, is important for assessing an electrolyte performance. In this study, the uniform mass transfer to the electrode surface in the modified Mohler cell is provided by flowing the electrolyte through the cell parallel to the electrodes (Fig. 2). The two side walls of rectangular cell are therefore open to let the forced electrolyte flow.

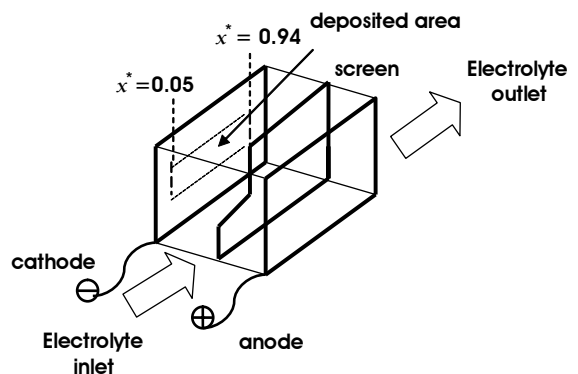
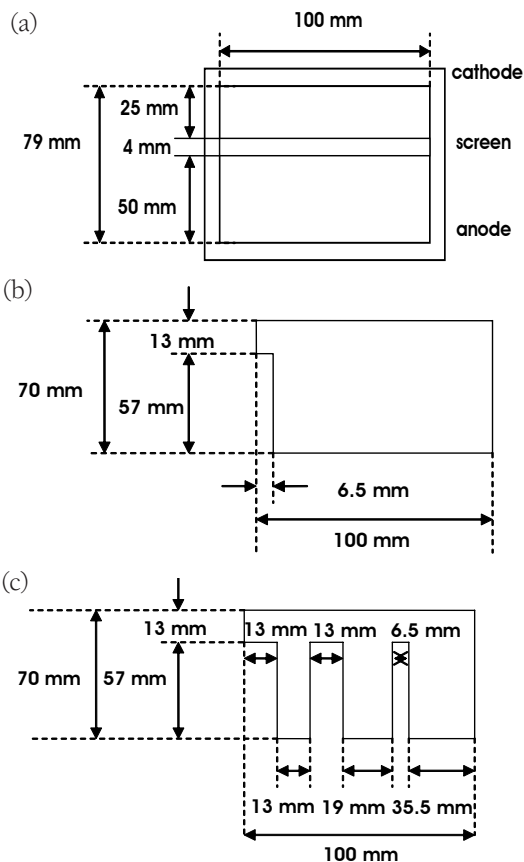


Fig 2. The modified Mohler cell with forced electrolyte flow.

A schematic diagram of the Mohler cell<sup>8</sup> is shown in Fig. 3. It is a rectangular cell with a plastic screen placed between the cathode and anode, and perpendicular to the potential direction.

In the Mohler cell, the current distribution depends on the shape of the insulator. One insulator with a single slit along the side of the screen, gives a logarithmic current distribution along the cathode, while the other insulator containing three slits provides a linear current distribution. As shown in Fig. 3 (a), the screen was placed between the electrodes at 25 mm from the cathode, and 50 mm from the anode. The different insulating screens modify the electrical field along the two electrodes resulting in different types of current distribution on the electrodes.



**Fig 3.** Schematic of the Mohler cell. (a) Top view of the Mohler cell. (b) The screen with one slit along the side. (c) The screen with three slits.

**Experimental**

The electrolytic cell was designed like the traditional Mohler cell, except that this electrolyte flow was parallel to the electrode surface. Therefore, two side walls of the rectangular reactor were open.

As shown in Fig. 4, the experimental device comprised a 10-liters electrolytic tank (T), a centrifugal pump (P), a electrolytic cell, 79 mm height, 70 mm width and 100 mm long (C) and two 0.7-m-long adaptive channels (A) to pass electrolyte from the circular section of the pipes to the rectangular section of the cell and to ensure a fully developed flow in the cell.

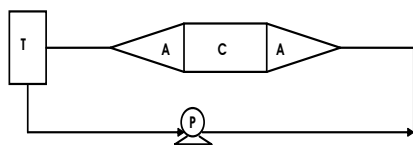


**Fig 4.** Electrolyte cell configuration. (T) electrolytic tank; (A) adaptive channel; (C) electrolytic cell; (P) centrifugal pump.

The electrical circuit included a 10 A - 30 V., regulated DC power supply ZS 3205 (Philips). The cathode was a stainless steel sheet. The anode was a Ti/RuO<sub>2</sub> grid with an active area of 52.5×10<sup>-4</sup> m<sup>2</sup>. The cathode was a 70×10<sup>-4</sup> m<sup>2</sup> stainless steel sheet with the deposited area of 27 ×10<sup>-4</sup> m<sup>2</sup> (Fig. 5).

Analytical reagents were used to prepare the electrolyte solutions. The copper sulfate bath was composed of 37 g.dm<sup>-3</sup> Cu<sup>2+</sup> and H<sub>2</sub>SO<sub>4</sub> was used for adjust pH at 4. The solutions were kept at 25 °C. Copper deposits were obtained at constant current densities at 0.22, 0.30 and 1.11 mA.mm<sup>-2</sup>. The electrolytic flow rate was 0.7 dm<sup>3</sup>.s<sup>-1</sup>.

The current density is related to the mass deposit through Faraday's law.

$$\frac{i(x^*)}{i_{ave}} = \frac{nFW(x^*)}{Mt}$$

$$x^* = \frac{x}{h} \quad (x^* \text{ is the dimensionless length}) \quad (2)$$

where M is the atomic weight of copper (63 g.mol<sup>-1</sup>), n is valence, F is Faraday's constant (96484.6 C.mol<sup>-1</sup>), t is time (s), and W is the deposit weight (g).

The deposited area (27 ×10<sup>-4</sup> m<sup>2</sup>) corresponds to the upper part of the cathode because previous works<sup>9</sup> have shown that uniform deposits are obtained in this area (by optimizing the deposited zone that provides uniform deposited layer). Before the deposition process, the cathode plate was coated by a resin, except on the deposited area. After electrolysis, the copper content on the deposited area was protected by resin and divided into 9 samples of the same surface area (samples 1 to 9). The resin of the sample part 1 was first to be removed using trichloroethylene then this was

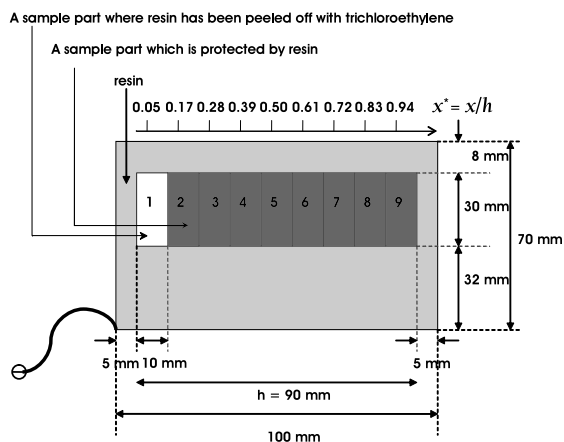


**Fig 5.** Partition of copper deposit on cathode surface of the Mohler cell.

followed by the dissolution of the copper deposit in nitric acid and analyzed using atomic absorption spectrometry. This process was repeated for all 9 samples, as seen in Fig. 5.

### Rotating Cylinder Hull Cell

The Rotating Cylinder Hull (RCH) configuration (Fig. 6) was used for the investigation of galvanostatic deposition investigation where the working electrode was a nickel cylinder (15 mm in diameter). The rotating rate was controlled by a servo-control of a rotating electrode (model EDI 101 Radiometer, Copenhagen). An insulating cylindrical wall with a diameter of 53 mm was placed around the electrode in order to induce a controlled non-uniform primary current distribution along the electrode length. The counter electrode was a Pt/RuO<sub>2</sub> grid (78 mm in diameter) placed around the outside of the insulating tube. The current and potential was controlled by a DEA 332 Digital Electrochemical analyzer (Radiometer), piloted by the software Master 2<sup>®</sup>. The reference electrode was a saturated calomel electrode.

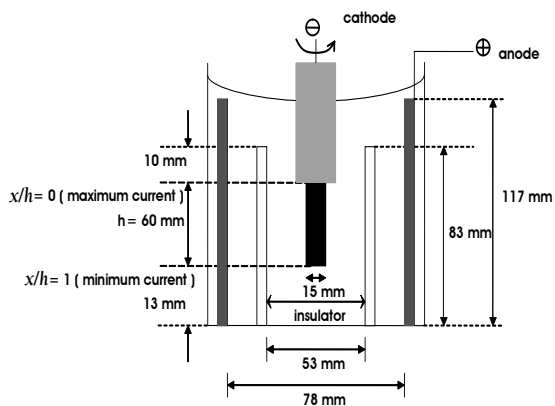


Fig 6. A schematic diagram of the conventional RCH cell.

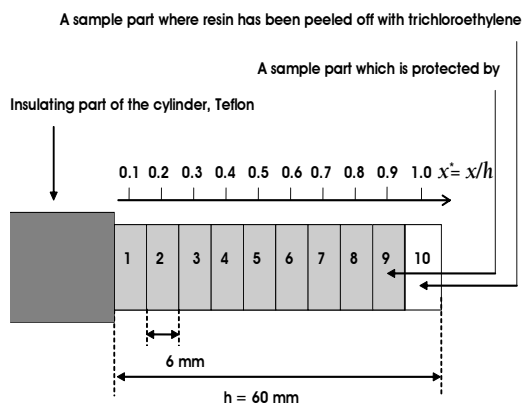


Fig 7. Partition of copper deposit on the cylinder cathode of the RCH cell.

### Experimental

Deposition was performed galvanostatically at average current densities ranging from  $0.71 \times 10^{-2}$  mA.mm<sup>-2</sup> to  $9.2 \times 10^{-2}$  mA.mm<sup>-2</sup> corresponding to Wagner numbers between 0.4 and 0.03 (Table 1). The rotation speed was performed at 1250 rpm. All deposits were plated at a constant temperature of 24 °C. Prior to deposition, the nickel cylinder cathode was polished with sandpaper and rinsed with distilled water. The electrolyte was standard to the one used for the modified Mohler cell investigation. The cathodic Tafel constant was found to be  $\beta_c = 30.8$  mV and the electrolyte resistance was  $0.187 \text{ } \Omega \cdot \text{m}$ . The time duration was increased when the current densities decreased in order to keep convenient accuracy for the measurement of the copper deposition rate.

After electrolysis, the copper content on cylinder cathode were protected by resin and cut into give a number of 10 samples of the same surface area (samples 1 to 10). The resin of the sample part 10 was first to be removed using trichloroethylene then was followed by the dissolution of the copper deposit in nitric acid and analyzed using atomic absorption spectrometry. This process was repeated for all 10 samples, as seen in Fig. 7.

A high copper concentration ( $37 \text{ g} \cdot \text{dm}^{-3}$ ) was used to minimize the influence of mass transport. Current efficiency for the copper deposition (measured by

Table 1. Operating conditions for RCH tests.

$i_{ave}$ (mA mm <sup>-2</sup> )	$Wa$	$t$ (s)
$9.20 \times 10^{-2}$	0.03	726
$4.58 \times 10^{-2}$	0.06	726
$2.76 \times 10^{-2}$	0.1	2358
$1.41 \times 10^{-2}$	0.2	2358
$0.71 \times 10^{-2}$	0.4	10800

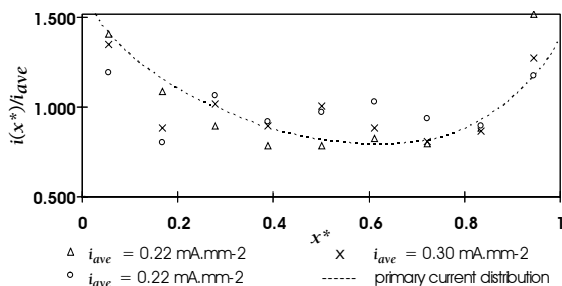
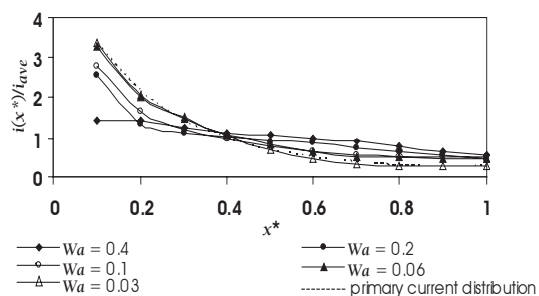


Fig 8. Dependence of dimensionless current density distribution versus dimensionless distance at various average current densities, and comparison with theoretical results corresponding to a primary current distribution.



**Fig 9.** Dimensionless current density ( $i(x^*)/i_{ave}$ ) represented as a function of the dimensionless length ( $x^*$ ) along the cathode at various average current densities corresponding to different Wagner numbers.

weight gain experiments) was found to be approximately 100 % for all deposits.

## RESULTS AND DISCUSSION

### Current Distributions in the Mohler Cell

In order to verify the linear current distribution in the Mohler cell, the three slits screen was used. Fig. 8 shows the experimental dimensionless current density ( $i(x^*)/i_{ave}$ ) versus the dimensionless length ( $x^* = x/h$ ) along the distance of the cathode. The observed current density along the length of the cathode decreases from the inlet to the mid point of the cell, and increases from this point to the outlet.

The variation of current versus the reduced distance does not produce a linear current distribution. The local current density is found to vary within a range from about 0.18 to 1.33 mA.mm<sup>-2</sup> for average deposition current densities ranging from 0.22 to 1.11 mA.mm<sup>-2</sup>. It was found that the ratio of the maximum (obtained at  $x^* = 0.05$ ) to the minimum dimensionless current density (obtained at  $x^* = 0.05$  and 0.5, respectively) was only 2. Thus, the current variation at the cathode does not cover a wide range of current distribution for each average current studied. In addition, there is an edge effect at the inlet and outlet of the cathode, seen as the increased current at  $x^* = 0.05$  and 0.94, respectively.

To further understand this results of this kind of current distribution behavior in the modified Mohler cell, a two-dimensional simulation of the primary current distribution in this cell was made. A more detailed discussion on assumptions and limitation of the model in this study has been given elsewhere<sup>10,11</sup> and is identical to the previous publication<sup>12</sup>. The comparison between experimental data and the primary current distribution derived by employing the Laplace's equation is also shown in Fig. 8. The simulation results confirm that the current variation is not linear,

and that border effects are also observed. Results do not present an obvious difference between the maximum and the minimum ends of the dimensionless current density, which are due to the border effects. The simulation result presents a little higher value at  $x^* = 0.05$  compared to those obtained at  $x^* = 0.94$ , but the difference between these values is low. In other words, the border effects are higher than slits effects.

The border effects are attributed to the modification of the configuration of the classical Mohler cell by putting out the side walls of rectangular reactor to let the electrolyte flow conveniently. Therefore, the current not only flows through to the slit but can also to the slit's border, resulting the loss of current at the inlet and outlet of the electrode. Consequently, the cell could not provide a wide current distribution range, resulting in the production of a non-linear current distribution and border effects.

This modified Mohler cell is thus not useful as a screening tool or to control the quality of the bath compared with the traditional Hull cell or the classical Mohler cell. Further investigations have been performed with the other type of plating test to obtain more evenly produced current distributions along the cathodic length. Rotating Cylinder Hull cell (RCH) described recently in the literature and developed by Madore et al<sup>5,7,13</sup> has been employed.

### Verification of Current Distribution in RCH

In Fig. 9, the experimentally determined dimensionless current densities ( $i(x^*)/i_{ave}$ ) are represented as a function of the dimensionless length ( $x^* = x/h$ ) along the cathode. High  $Wa$  numbers are indicative of a more uniform current distribution.

The variation of current versus the dimensionless distance does not present a border effect, the local current density was found to vary within a range from about  $3.4 \times 10^{-2}$  to 0.4 mA.mm<sup>-2</sup> for average deposition current densities ranging from  $0.71 \times 10^{-2}$  to  $9.2 \times 10^{-2}$  mA.mm<sup>-2</sup>. The ratio of the maximum to the minimum current (obtained at  $x^* = 0.05$  and 0.94, respectively) is 7, which is 3.5 times higher than that obtained in the Mohler cell. The variation thus covers a wider current distribution range than the experiments performed with the modified Mohler cell.

The theoretical primary current distribution, dashed line, for the RCH cell (Fig. 9) can be represented by the following analytical expression<sup>13</sup>.

Good agreement was found between the empirical curve and the experimental curves for Wagner numbers ( $Wa$ ) ranging from 0.03 to 0.06. Therefore, it can be concluded that experiments performed with  $Wa$  number lower than 0.03 are representative of current distributions that are nearly primary. However,  $Wa$  numbers higher than 0.4 are representative of current

$$\frac{i(x^*)}{i_{ave}} = \frac{0.652 - 0.609(x^*)}{\{0.0209 + (x/h)^2\}} + 2.66 \times 10^{-3} \times \exp\{4.53(x^*)\} \quad (3)$$

$$x^* = \frac{x}{h}$$

distributions that are secondary. The latter is clearly differentiated from the primary current distribution calculated from the empirical equation (3). In this case, the current distribution is much more uniform than those observed at lower Wagner number.

### Copper Plating Involving a Mass Transport Limited Step

The mass transfer effects were investigated in the RCH cells using an average current density of  $9.2 \times 10^{-2} \text{ mA} \cdot \text{mm}^{-2}$ , at varied rotation rates ranging from 250 to 2500 rpm. Deposition times were 720 seconds at a temperature of 22 °C. The electrolyte contained a low copper concentration ( $1.6 \text{ g} \cdot \text{dm}^{-3} \text{ Cu}^{2+}$ ), in order to facilitate mass transport control of the copper deposition reaction.

Fig. 10 shows the variation of dimensionless current density distribution as a function of dimensionless distance at various rotating speeds. At a speed of 1250 and 2500 rpm, the variation of current densities yield current distributions that are nearly primary, resulting in good agreement when compared with the experimental results with those from the model. However, at 250 rpm, current distribution is more uniform and corresponds to a secondary current distribution (clearly differentiated from the empirical curve and more uniform). Consequently, the effect of mass transport could be observed at the speed 250 rpm. Moreover, the current efficiency of the rotating speed at 250 rpm is less than 100 %.

### CONCLUSION

Two kinds of cells have been tested in order to

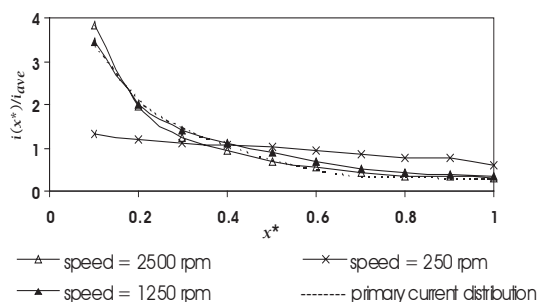


**Fig 10.** Variation of dimensionless current density distribution versus dimensionless distance at various rotating speeds.

determine the best device to characterize electroplating baths. The first is the modified, flow-through Mohler cell, this cell was designed, built and tested for copper deposition from acid baths. By positioning an insulating screen between the parallel electrodes, the electric field was distorted to produce a distribution of currents across the cathode surface of Mohler cell. In this cell, mass transfer was imposed by the electrolyte flow parallel to the electrodes, and the experiments performed with this cell can be used to simulate electroplating under industrial hydrodynamic conditions, especially for modern types of industrial cells where mass transfer is imposed by circulation. With exception of the edge effects at the inlet and outlet of the cathode, the ratio of the maximum to minimum current densities studied was low, ranging from 1 to 2, this fact was confirmed by simulating a primary current distribution. However, it was concluded that this cell is not very useful as a bath control cell, in which a large range of current densities must occur. The large area cathode allows study of the influence of the current on the deposit structure.

On the other hand, Rotating Cylinder Hull cell, RCH has been tested using the same electrolyte. It has been shown that experimental results agree well with the empirical formula determined for primary current distribution. In this case the ratio of the maximum to the minimum current (7) covers wider range of current distribution than those observed from the modified Mohler cell. Therefore, this device constitutes a very pertinent piece of equipment to bath control.

### ACKNOWLEDGEMENTS

The author gratefully acknowledge the valued help from Dr. Bernard Fenouillet of INPT, ENSIACET for his assistance with experimentation. This work was financially supported by the Thailand Research Fund (Thailand) and by the French Embassy of Thailand.

### NOMENCLATURE

$F$	Faraday's constant, $96484.6 \text{ C} \cdot \text{mol}^{-1}$
$h$	cathode length, mm
$i_{ave}$	average current density, $\text{mA} \cdot \text{mm}^{-2}$
$k$	electrolyte conductivity, $\text{S} \cdot \text{m}^{-1}$
$L$	characteristic length of the system, mm

$M$	atomic weight of copper, 63 g.mol <sup>-1</sup>
$n$	number of electron transfer (eq uivalent. mol <sup>-1</sup> )
$t$	time, s
$W$	deposit weight, g
$x^*$	dimensionless length
$(i(x^*)/i_{ave})$	dimensionless current density
$W\alpha$	Wagner number

Greek characters

$\eta$	overpotential, mV
$\rho$	electrolyte resistance, 0.187 $\Omega$ .m
$\beta_c$	cathodic Tafel constant, 30.8 mV

## REFERENCES

- Hull RO (1939) *J. Am. Electroplat Soc.* **27**, 52-60.
- Graham AK and Pinkerton HL (1963) A cell for high-speed plating evaluations. *Tech. Proc. Am. Electroplaters Soc.* **50**, 135-8.
- Kadija I, Abys JA, Chinchankar V and Straschil HK (July, 1991) Hydrodynamically Controlled "Hull Cell". *Plat. and Surf. Fin.* **78**, 60-7.
- Po-Yen Lu (Oct., 1991) The Lu Cell-A Hull Cell With a Rotating Cathode. *Plat. and Surf. Fin.* **78**, 62-5.
- Madore C and Landolt D (Nov., 1993) The rotating cylinder Hull cell: Design and application. *Plat. and Surf. Fin.* **80**, 73-8.
- Pinkerton H L (1984) Current and metal distributions in Electroplating Engineering Handbook, pp 461-73. Van Nostrand Reinhold, NY
- Madore C, Matlosz M and Landolt D (1992) Experimental investigation of the primary and secondary current distribution in a rotating cylinder Hull cell. *J. Appl. Electrochem.* **22**, 1155.
- Lacourcelle L (1997) Information à l'usage du concepteur, fiche 24. Librairie du traitement de surface, Paris.
- Faust E (Jul., 2001) Stage Recherche 2<sup>ème</sup> année, ENSIACET INP, Toulouse
- Dupuy F, Vergnes H, Fenouillet B and Duverneuil P (2003) Numerical simulation of the current distribution in different geometries. ECCE 4<sup>th</sup> European congress of chemical engineering. Granada Spain, 21-5 Sep 2003.
- Dupuy F, Vergnes H, Fenouillet B and Duverneuil P (2003) Modélisation de la distribution de courant dans les reacteurs électrochimiques. Saint-Nazaire, 9 - 11 Sep 2003.
- Matlosz M, Creton C, Clerc C and Landolt D (1987) Secondary current distribution distribution in a Hull cell. Boundary element and finite element simulation and experimental verification. *J. Electrochem. Soc.* **134**, 3015-21.
- Madore C, West AC, Matlosz M and Landolt D (1991) Design Considerations for a cylindrical hull cell with forced convection. *Electrochim Acta* **37**, 69-74.